Published in final edited form as:
J Exp Biol. 2008 May ; 211(Pt 10): 1594–1602. doi:10.1242/jeb.017244.

Synergy and specificity of two Na+–aromatic amino acid symporters in the model alimentary canal of mosquito larvae

Bernard A. Okech[*], **Ella A. Meleshkevitch**[†], **Melissa M. Miller**, **Lyudmila B. Popova**[‡], **William R. Harvey**, and **Dmitri Y. Boudko**[§,†]
The Whitney Laboratory for Marine Bioscience, University of Florida, 9505 Ocean Shore Boulevard, St Augustine, FL 3208, USA

SUMMARY

The nutrient amino acid transporter (NAT) subfamily is the largest subdivision of the sodium neurotransmitter symporter family (SNF; also known as SLC6; HUGO). There are seven members of the NAT population in the African malaria mosquito *Anopheles gambiae*, two of which, AgNAT6 and AgNAT8, preferably transport indole- and phenyl-branched substrates, respectively. The relative expression and distribution of these aromatic NATs were examined with transporter-specific antibodies in *Xenopus* oocytes and mosquito larval alimentary canal, representing heterologous and tissue expression systems, respectively. NAT-specific aromatic-substrate-induced currents strongly corresponded with specific accumulation of both transporters in the plasma membrane of oocytes. Immunolabeling revealed elevated expressions of both transporters in specific regions of the larval alimentary canal, including salivary glands, cardia, gastric caeca, posterior midgut and Malpighian tubules. Differences in relative expression densities and spatial distribution of the transporters were prominent in virtually all of these regions, suggesting unique profiles of the aromatic amino acid absorption. For the first time reversal of the location of a transporter between apical and basal membranes was identified in posterior and anterior epithelial domains corresponding with secretory and absorptive epithelial functions, respectively. Both aromatic NATs formed putative homodimers in the larval gut whereas functional monomers were overexpressed heterologously in *Xenopus* oocytes. The results unequivocally suggest functional synergy between substrate-specific AgNAT6 and AgNAT8 in intracellular absorption of aromatic amino acids. More broadly, they suggest that the specific selectivity, regional expression and polarized membrane docking of NATs represent key adaptive traits shaping functional patterns of essential amino acid absorption in the metazoan alimentary canal and other tissues.

Keywords

insect; mosquito; essential amino acid; nutrient amino acid transporter; NAT; co-transporter; phenylalanine; tryptophan; monoamine neurotransmitter; malaria; *Anopheles gambiae*

INTRODUCTION

The African malaria vector mosquito *Anopheles gambiae* belongs to a group of tropical culicids that can rapidly develop in freshwater aquatic environments. These adaptations

[§]Author for correspondence (dmitri.boudko@rosalindfranklin.edu).
[*]Present address: The Whitney Laboratory and Emerging Pathogens Institute and Department of Epidemiology and Statistics, University of Florida, Gainesville, FL 32610, USA
[†]Present address: Department of Physiology and Biophysics, Rosalind Franklin University, School of Medicine, North Chicago, IL 60064, USA
[‡]Present address: A. N. Belozersky Institute, Moscow State University, Moscow 119899, Russia

require efficient absorption of nutrients, including 10 essential amino acids (reviewed in Clements, 1992). Accordingly, interruption of an essential amino acid absorption mechanism in mosquito larvae could be employed to reduce the vector component of disease transmission in endemic areas. However, safe and effective application of this attractive strategy requires comprehensive understanding of specific and universal properties of essential amino acid transport in target and key risk-of-exposure metazoan organisms.

Earlier studies documented the active absorption of essential amino acids in mosquitoes (Uchida et al., 2003; Uchida et al., 2001; Uchida et al., 1990) and other insects (Caccia et al., 2005; Castagna et al., 1997; Giordana et al., 1989; Nedergaard, 1972; Wolfersberger, 2000). Using genome data mining in combination with comparative phylogenetic analysis of transporters in selected organisms with published genomes, we identified and compared key families of secondary transporters that contribute to the amino acid traffic network in metazoans (Boudko et al., 2005c). Each identified family provides a unique but complementary part in the contiguous traffic and balance of amino acids; however, the molecular identity and phylogeny of a core mechanism for active absorption of essential amino acids remained uncertain. An intriguing paralogous expansion of ‘orphan’ transporters was identified among insect members of the sodium neurotransmitter symporter family (SNF; also known as, solute carrier family 6; SLC6) (Boudko et al., 2005a; Boudko et al., 2005b; Boudko et al., 2005c). Based on their phylogenetic closeness with characterized neutral amino acid transporters – two from the tobacco hornworm larva, *Manduca sexta*, msKAAT1 (Castagna et al., 1998) and msCAATCH1 (Feldman et al., 2000); and one from the yellow fever mosquito *Aedes aegypti*, aeAAT1 –we anticipated a homologous physiological role for other members of the identified group (Boudko et al., 2005a). All of the identified genes appear to encode moderately conserved, monovalent cation–amino acid symporters, which mediate the uptake of a set of neutral amino acids, almost all of which are essential for insects and other metazoans. Moreover, this insect-specific cluster neighbors a cluster of B^0 system transporters that mediates the absorption of a broad spectrum of neutral amino acids in mammals (Broer et al., 2006a); it also neighbors a set of orphan *Caenorhabditis elegans* transporters, several of which are extensively transcribed in the worm alimentary canal (www.wormbase.org). The entire group, designated as nutrient amino acid transporters (NATs), represents a functionally segregated subfamily of SNF (SLC6) (Boudko et al., 2005a; Boudko et al., 2005b; Boudko et al., 2005c). *Drosophila melanogaster*, *An. gambiae* and *Ae. aegypti* have 7, 6 and 9 (possibly +1) NAT members, respectively, demonstrating strong paralogous diversification and variation in gene numbers. This observation suggests that a rapid duplication and functional specialization of NAT members occurs (Boudko et al., 2005a). The retention and consistent expansion of paralogous NATs seen from bacteria to metazoans imply the conservation of a fundamental role of these transporters during metazoan evolution. The NAT-SLC6 population appears to have evolved as an integrated system that performs high-throughput absorption of essential amino acids and their derivatives (Boudko et al., 2005c). Recently, we have cloned and characterized two NATs with unique transport properties from *An. gambiae* larval midgut (Assis et al., 2004; Boudko et al., 2005b; Meleshkevitch et al., 2006). Both transporters mediate Na^+- or K^+-coupled voltage-gradient-driven absorption of specific aromatic substrates. However, AgNAT6 (AAT07965) preferably absorbs tryptophan and indole-branched substrates, whereas AgNAT8 (AAN40409) preferably absorbs phenyl-branched substrates. To determine the physiological significance of such an extraordinary specialization we examined the relative distribution of these aromatic NATs in the model system of the alimentary canal from mosquito larvae. In addition, we analyzed the assembly and docking of the NATs in a heterologous expression system, *Xenopus laevis* oocytes.

MATERIALS AND METHODS

Procurement and rearing of mosquitoes

Anopheles gambiae Giles *sensu stricto* (Diptera, Culicidae, G3 strain) eggs were obtained from the Malaria Research and Reference Reagent Resource Center (MR4) of the Centers for Disease Control and Prevention (CDC) in Atlanta, Georgia, USA (Cat. No MRA-122). The eggs were used immediately after overnight shipment. The larvae were raised according to a standard maintenance protocol which was developed at the Whitney Laboratory for Marine Bioscience, University of Florida and approved by the Bureau of Entomology and Pest Control, Florida Department of Agriculture and Consumer Services. Briefly: eggs were hatched in deionized water (DW) and larvae were fed every 2 days with a mixture of one part yeast and three parts Wardley® Tetramin fish flakes which contains a sufficient supply of mineral ions. The rearing medium was changed every 3 days by replacing about 90% of the volume with fresh DW. Larval mosquitoes were used at the third to early fourth instar developmental stage.

Antibody preparation

Antigen motif selection was based on antigenicity plots and the putative 3D structure of AgNAT6 and AgNAT8 that were cloned and sequenced in our laboratory (accessions AAT07965 and AAN40409). Selected motifs were unique relative to each other, to the rest of AgSLC6 and to the *Anopheles* protein database. Two synthetic oligopeptides, EQSLPRDRSLVRRMFDNVFS and GPIDPATHYEYKKFIDED, corresponding to the C-terminal 20 and 18 amino acids of AgNAT6 and AgNAT8, respectively, were synthesized at a 20 micromolar scale, emulsified in Freunds complete adjuvant and used according to a 90-day immunization protocol (Open Biosystems, Huntsville Alabama, USA; operating in accordance with animal use regulations). Antibodies were prepared by immunizing rabbits with these synthetic oligopeptides conjugated to keyhole lympet hemocyanin (KLH). A separate rabbit antibody with low binding of pre-bleed sera as tested by ELISA was selected for each immunization. The immunization series included a primary injection, 14th day first boost and 28th day second boost injections of oligopeptides. Bleeds were collected every 28 days after the primary immunizations. The crude sera were affinity purified against the respective immunizing peptides.

Heterologous expression of AgNATs in *Xenopus* oocytes

Oocytes were collected from live *Xenopus laevis* Daudin (Xenopus Express Inc., Brooksville, FL, USA) under sterile aseptic conditions as approved by the University of Florida (IACUC 6032). Frogs were anesthetized by immersion in ice-cold 0.1% tricaine solution and 1 cm cuts were made on the lower ventral abdomen from which eggs were harvested; operated frogs were euthanized according to the approved protocol. Apparent stage V–VI oocytes were isolated from egg clusters after treatment with a 2% collagenase solution in Ca^{2+}-free ND96 medium (96 $mmol \cdot l^{-1}$ NaCl, 2 $mmol \cdot l^{-1}$ KCl, 1 $mmol \cdot l^{-1}$ $MgCl_2$, 10 $mmol \cdot l^{-1}$ Hepes, pH 7.4). Separated oocytes were conditioned for a few hours in Ca^{2+} trace ND96 before being used in experiments. cRNA was prepared from pXOOM plasmids of NAT clones using a high yield capped RNA transcription kit, mMESSAGEmMACHINE® (Ambion, Foster City, CA, USA) as described previously (Boudko et al., 2005a; Meleshkevitch et al., 2006). Approximately 20 ng cRNA was injected into each oocyte using a capillary glass micropipette attached to a Nanoliter 2000 injector (WPI, Sarasota, FL, USA). Oocytes were incubated at 16°C for 4 days after which they were evaluated for amino acid transport activity using a standard two-electrode voltage clamp technique (Meleshkevitch et al., 2006) followed by immunolabeling.

Isolation of membranes from larvae and oocytes

Cell membrane fractions were isolated from *An. gambiae* larvae and *X. laevis* oocytes that had been injected with either distilled water (control), AgNAT6 or AgNAT8 cRNA according to a modified Hill protocol (Hill et al., 2005). Briefly, tissues were suspended in homogenization buffer (HB; 250 mmol·l^{-1} sucrose, 5 mmol·l^{-1} $MgCl_2$, 10 mmol·l^{-1} Hepes, pH 7.4) containing a 1:1000 dilution of protease inhibitor cocktail (Sigma-Aldrich, St Louis, MO, USA). Larvae and oocytes were homogenized using a glass Dounce or plastic pestle with a disposable 1.5 ml tube, respectively, followed by ultrasound agitation. Homogenates were centrifuged at 500 ***g*** for 5 min and the supernatant was recovered. Pellets were resuspended in the same volume of HB and processed as before. The second supernatant was combined with the first one and the crude membrane suspension was overlaid on a discontinuous sucrose gradient consisting of 20% sucrose–HB and 50% sucrose–HB, and centrifuged at average Relative Centrifugal Field (RCF_{av}) 111000 ***g*** at 4°C for 30 min using a Beckman SW-41 rotor. The layer visible at the gradient interface, representing the membrane fraction, was collected using a micro-syringe, diluted threefold in HB, and recovered by centrifugation at RCF_{av} 111000 ***g*** at 4°C for 30 min. The resulting membrane pellet was resuspended in HB with added protease inhibitors and quantified for protein content using the Bio-Rad protocol (Bradford, 1976).

SDS-PAGE and western blot analysis

Protein samples were treated with NuPAGE® LDS sample buffer (Invitrogen, Carlsbad, CA, USA) and β-mercaptoethanol and heated at 70°C for 10 min. Samples (4 μg per lane) were separated under reducing conditions on a denaturing 4–12% Bis–Tris polyacrylamide gradient gel. Separated proteins were blotted onto nitrocellulose membranes (0.22 μm; Millipore, Billerica, MA, USA) using a tank transfer system. Blots were stained with Fast Green to confirm equal loading and transfer and to visualize lane boundaries; then they were cut into strips for probing with various serum samples. Before being probed, blots were incubated in blocking buffer containing 5% non-fat dry milk powder (Carnation®) in Tris-buffered saline (TBS) for 1 h at room temperature. Blots were then incubated with AgNAT6 or AgNAT8 antibody at a dilution of 1:500 in 2% dry milk–TBS with 0.05% Tween-20 (TBST) overnight at 4°C. As a control, lanes with identical membrane samples were incubated with pre-immunization serum. Nitrocellulose membranes were washed in TBST and incubated with alkaline phosphatase-conjugated goat anti-rabbit IgG (Jackson ImmunoResearch, West Grove, PA, USA) diluted at 1:1000 in 2% dry milk–TBST for 1 h at room temperature and then washed in three changes of TBST for 10 min each, followed by one 10 min wash in TBS. Bound antibodies were detected by an alkaline phosphatase color precipitation reaction (Bio-Rad, Hercules, CA, USA).

Whole-mount immunolabeling

Oocytes were fixed in 4% paraformaldehyde (PFA) in 0.1 mol·l^{-1} PBS for approximately 3 h and rinsed with three changes of ice-cold PBS for 5 min each. Fourth instar larvae were immobilized in ice-cold PBS, injected with 4% PFA and dissected as described previously (Meleshkevitch et al., 2006). The protocols for immunolabeling of oocytes and larvae were similar. Fixed oocytes and larvae samples were permeabilized in 0.1% Triton X-100 in PBS (PBT) for 6–12 h at 4°C on a shaker. Next, the samples were incubated in blocking solution (BS; 2% normal goat serum, 1% bovine serum albumin in PBT) for 12–24 h at 4°C. The primary antibodies against AgNAT6 or AgNAT8 were then added at a dilution of 1:100 in BS and left at 4°C on a shaker for a further 24 h. The preparations were rinsed four times in BS for 30 min each, and incubated with Alexa Fluor 488-conjugated goat anti-rabbit (GAR) secondary antibody (Invitrogen) at a dilution of 1:800 in BS overnight at 4°C. Preparations were subsequently labeled with phalloidin–Rhodamine (Invitrogen; 1:250 in PBS) for 15

min at room temperature to visualize muscle actin, and with DRAQ-5 (Biostatus Limited, Shepshed, UK; 1:1000 in PBS) for 5 min to visualize cell nuclei. Then they were washed and mounted in 3:1 glycerol:PBS on microscope slides. To prepare a relative-fluorescence-intensity graph two selected images of whole-mount labeled preparations of AgNATs from identical fourth instar larval stages were scanned using the Plot Profile tool of the ImageJ 1.38 software package (http://rsb.info.nih.gov/). Apparent intensity values were copied to a SigmaPlot spreadsheet, normalized and used to generate a graph.

Frozen section immunolabeling

A surgically isolated and paraformaldehyde-fixed alimentary canal was incubated in a 30% sucrose–PBS solution for 12 h, saturated in TissueTek® embedding medium and mounted at −20°C on a cryostat base. Sections (15 μm) were prepared using a cryostat microtome. For immunolabeling, the sections were warmed at room temperature, resaturated and permeabilized in BS for 2 h. The slides were rinsed in PBT and incubated in a humidified chamber with primary antibodies (1:50 in PBT) for 4 h at room temperature. Sections were washed in PBT and incubated with Alexa Fluor 488-GAR secondary antibodies (Invitrogen; 1:500 in PBS) for 1 h at room temperature. Subsequently, preparations were washed and incubated with phalloidin–Rhodamine and DRAQ-5 as described above. Images of immunolabeling were acquired using a Leica laser scanning confocal microscope with laser excitation at 495 nm, 550 nm and 678 nm for fluorescein, Rhodamine and DRAQ-5, respectively. Scanned frame stacks were reconstructed as three-dimensional projections and selected planes were converted to BMP images and assembled into final plates using the Corel Draw X3 software package (Corel Corporation, Ottawa, ON, Canada).

RESULTS

Western blots of heterologously and *in situ* expressed AgNATs

Mosquito tissues or NAT-expressing oocytes were not labeled by pre-immune serum (Figs 1, 2). Post-immune crude or purified sera did not label water-injected control oocytes (data not shown). Labeling of blot membranes from heterologously expressing oocytes or midgut tissues with crude serum was completely blocked by prior treatment with excess of the synthetic NAT peptides used for the antibody production (data not shown). Serum (data not shown) and peptide-affinity purified antibodies against AgNAT6 and AgNAT8 reacted specifically with membrane fractions isolated from oocytes expressing AgNAT6 and AgNAT8 and membrane fractions from mosquito gut (Fig. 1). The labeling of blots revealed several major bands with electrophoretic migrations within a 51–110 kDa window, two of which approximately correspond to the calculated molecular masses for putative monomers and homodimers of the analyzed proteins (Fig. 1, arrowheads; theoretical pI/Mw are 6.85/72771.93 and 7.06/70233.05 for AgNAT6 and AgNAT8, respectively). Some scattering of the band migration pattern, typically corresponding to posttranslational glycosylations, was observed. Upper bands for AgNAT6 and AgNAT8 differ in apparent molecular masses, which may suggest the absence of heterodimers of those transporters in tissues (Fig. 1, asterisks; $N \geq 3$). Strong bands of smaller molecular mass were present in the membrane fractions from the heterologous expression system. These bands may reflect labeling of incomplete NAT fragments, which could form upon heterologous overexpression. Intense high molecular mass bands were also observed between putative monomer and homodimers bands in heterologously expressed but not in tissue samples. These bands may suggest accumulation of abnormal peptide associations, e.g. oligomerization of mature NATs with small molecular mass peptides such as the immature NAT fragments proposed above. The differences in electrophoretic migration of heterologous and tissue fractions were similar for AgNAT6 and AgNAT8 expression, suggesting generalization of the protein maturation process and escalation of maturation

problems upon heterologous overexpression. The upper band of a putative dimer represents the dominant form of AgNATs in epithelial tissue samples, whereas putative monomers and incomplete dimers were prevalent in the heterologously expressed samples.

Localization of heterologously expressed AgNATs in *Xenopus* oocytes

No notable staining was observed in control, water-injected oocytes (Fig. 2A,B) or in control preparations treated with pre-immune sera (data not shown). By contrast, *Xenopus* oocytes expressing AgNAT6 and AgNAT8 proteins for 3–4 days were specifically labeled with the transporter-specific antibodies. This labeling corresponds to efficient expression and predominant incorporation of the proteins in the oocyte plasma membranes (Fig. 2D,E,G,H). DW-injected control oocytes produced only minor responses on application of tryptophan or phenylalanine (Fig. 2C). By contrast, the immunolabeling of both AgNATs in *Xenopus* oocytes unequivocally correlates with functional expression, as determined by robust substrate-induced Na^+ currents (100% tests, $N \geq 20$ for each transporter; Fig. 2F,I) and previously reported radiolabel uptake of substrates (Meleshkevitch et al., 2006; Boudko et al., 2005b) (and data not shown). The aromatic amino-acid-induced responses revealed very specific, consistent Na^+ dependency, repeatable response kinetics and maximums of substrate-induced currents (Fig. 2F,I; summarized in Fig. 3). A diagram constructed by multi parameter sorting and Gaussian pick fitting of apparent transport efficiencies showed a very clear gain of specificity for indole- and phenyl-branched substrates in the AgNAT6 and AgNAT8 transporters (Fig. 3; right row; blue and red data sets, respectively).

Localization of AgNATs in whole mounts of the larval alimentary canal

Simple whole-mount preparations of mosquito larval alimentary canal provide unique opportunities to compare global patterns of spatial expression of the transporters. Steady-state patterns of immunolabeling in the larval alimentary canal were observed for both aromatic transporters (N=22; Fig. 4A,B). Fluorescence intensities were highest in the anterior and posterior regions of the alimentary canal, suggesting a synergetic contribution of both NATs to specific functions attributed to these epithelial regions (Fig. 4C). Nevertheless, upon closer comparison there were differences in the spatial distribution of the two transporters (Fig. 4). AgNAT6 was concentrated in the gastric caeca (GC) and central midgut (CM) as well as the anterior part of the posterior midgut (PMG; Fig. 4A). Less intense labeling was observed in the anterior midgut (AMG) and Malpighian tubules (MT). AgNAT8 antibodies produced intensive labeling in the salivary glands (SG), GC and PMG (Fig. 4B). Labeling of AgNAT8 was more intense in GC than in PMG, the opposite of AgNAT6 labeling in the same areas. In addition, labeling for AgNAT8 in the PMG was notably more posterior than that of AgNAT6 (Fig. 4C; N=8). AgNAT8 antibodies also labeled MT more intensely than those against AgNAT6. AgNAT8 antibody produced very weak labeling in the AMG and the large transitional region (CM) between AMG and PMG (N=6) in contrast to AgNAT6 antibodies which labeled this region very well. Specific labeling of AgNAT8 but not AgNAT6 was observed in the proximal portion of the MTs, which may reflect the distinct specialization of individual epithelial cells in this area (Fig. 4).

Localization of AgNATs in frozen sections of larval AC

The general pattern of immunolabeling in frozen sections (Fig. 5) corresponded well to the distribution of the two NATs in whole-mount preparations (Fig. 4) suggesting that the antibodies had permeated the tissues well in the latter. The higher resolution analysis of frozen sections was sufficient to determine intracellular distribution and plasma membrane localization of the aromatic AgNATs within epithelial tissues. Specific polar sorting of the transporters was found in both posterior and anterior regions of the larval alimentary canal. In PMG both transporters were most prevalent in columnar cell apical membranes. In AMG

and CM labeling was distinct in both apical and basal membranes of the epithelial cells. The labeling intensity was higher at the apical pole of AMG and CM, with each transporter differing with respect to intensities and spatial profiles (Fig. 5). The SG cells showed strong expression and uniform basal localization of both transporters (N=5). By contrast, in GC AgNAT6 was predominantly associated with the apical membrane whereas AgNAT8 was associated with both apical and basal membranes, with higher intensity in the latter. AgNAT8 was also strongly expressed in basal membranes of the cardia and in apical membranes of the principal cells of the proximal MT.

DISCUSSION

The *Plasmodium falciparum* malaria vector, *An. gambiae* is emerging as an important genomic and disease vector biology model (Holt et al., 2002; Linser et al., 2007). The alimentary canal epithelium in mosquito larvae consists of several thousands of large cells that mediate mineral ion balance, digestion, nutrient collection and metabolic waste emission. Thus it provides distinctive advantages for the study of the integrative and cellular basis of mineral ion and pH balances (Boudko et al., 2001a; Boudko et al., 2001b; Clark et al., 2007; Okech et al., 2008) as well as absorption of essential amino acids (Boudko et al., 2005a; Boudko et al., 2005b; Boudko et al., 2005c). It has an explicit regional pattern of functional specialization and provides an outstanding opportunity for parallel studies of molecular, cellular and systemic aspects of various membrane transporters (Boudko et al., 2005a; Meleshkevitch et al., 2006; Rheault et al., 2007).

Specificity of aromatic NATs in the amino acids traffic network

Each cell in metazoan organisms depends on the enduring supply of essential amino acids. Central to this supply network are the active initial absorption of these nutrients through apical membranes of the alimentary canal epithelial cells and their active re-absorption *via* plasma membranes of other cells (Boudko et al., 2005c; Broer, 2002). NAT-SLC6 members (a.k.a. B^0 system transporters) mediate this absorption by coupling uphill transport of the essential amino acids to downhill co-transport (symport) of alkali metal cations that is driven by ionic transmembrane electrochemical gradients (Boudko et al., 2005a; Broer et al., 2006a). This secondary active absorption of essential amino acids in insects is conducted by B^0 system-like transporters with specific substrate profiles. For example, AgNAT6 and AgNAT8, display little overlap in substrate spectra (Fig. 3). Both transport aromatic substrates but AgNAT6 translocates indole-branched substrates whereas AgNAT8 transports phenyl-branched substrates (Fig. 2). Duplication and specialization of aromatic NATs along with balanced relative expression can enhance primary absorption from midgut lumen and can provide for more precise cellular distribution of aromatic amino acids. Similar duplication and specialization of aromatic NATs in parallel with the extinction of complex, energy-consuming pathways for the synthesis of the aromatic substrates appears to be a key trade-off in the evolution of heterotrophy; however, it raises the question: exactly how do organisms provide and regulate NATs in response to metabolic demands in specific organs, tissues and cells?

Synergy of aromatic NATs in aromatic substrate absorption

The indole- and phenyl-branched amino acid transporters, AgNAT6 and AgNAT8, respectively, share high expression and apical location in the PMG. In this area the final stage of protein digestion produces elevated concentrations of free amino acids. The apical membranes of PMG cells have very long, densely packed microvilli which appear in light micrographs as a brush border (Clements, 1992; Zhang and Nichols, 1994) and which greatly expands the absorptive surface area. Although significantly higher transcript concentrations of AgNAT6 and AgNAT8 were detected in PMG by *in situ* hybridization

(Boudko et al., 2005a; Meleshkevitch et al., 2006), there was no direct evidence that the active nutrient amino acid transport mechanism is restricted to the apical membranes there. We provide here the first solid proof that two NAT members of the SLC6 family are expressed in the apical membranes of PMG in a pattern which suggests strongly that NATs act in synergy to ensure complete and effective apical absorption of nutrient aromatic amino acids. The results also suggest that the PMG is a primary site for the initial absorption of essential aromatic amino acids. In a broader sense, the synergy between AgNATs 6 and 8 suggests that they play universal, complementary role as essential substrate providers (Boudko et al., 2005a). This increased transcription and expression of aromatic NAT transporters in the PMG most likely corresponds to a gain of function and/or increased turnover of the proteins. Similar, elevated PMG transcriptions were found for other AgNATs and a few NATs from different dipteran species, e.g. *Ae. aegypti* and *D. melanogaster* (Boudko et al., 2005b; Meleshkevitch et al., 2006; Thimgan et al., 2006). Several members of the mammalian NAT subfamily (Boudko et al., 2005a; Broer, 2006; Hoglund et al., 2005) that is adjacent to the insect NAT cluster (Boudko et al., 2005a) are highly expressed in posterior parts of the mammalian alimentary canal (Bohmer et al., 2005; Broer et al., 2006b) and have been shown to dock in apical membranes of absorptive epithelia of kidney and small intestine (Romeo et al., 2006; Verrey et al., 2005). Collectively, these data support the hypothesis that the NAT-SLC6 group is evolving universally across the animal kingdom and providing a mechanism for the active absorption of essential amino acids from the digestive tract lumen across the plasma membranes of its epithelial cells. Based on the variety of substrates for individual, characterized transporters (e.g. aromatic AgNATs presented here) we propose that different members of the NAT SLC6 subfamily evolved distinct patterns of selectivity and suggest that the entire group appears to be evolving and working in synergy to ensure comprehensive absorption of a required set of essential amino acid substrates.

Benefits from NATs duplication and morphological segregation

The results presented here raise two questions inherent to NAT regulation. (1) Why do mosquitoes possess separate, selective transporters for indole- and phenyl-branched substrates whereas mammals appear to absorb both of these substrate groups *via* more universal transport mechanisms such as the broad substrate spectra NATs of system B^0 transporters? The apparent benefit of such duplication is a reduction of substrate competition for a single transporter. Mammalian transporters may operate in a contiguous mode, clearing essential amino acids one by one in successive regions of the relatively long intestine. By contrast, absorptive regions in the larval alimentary canal are only 2–3 mm long and the absorption window is open but a brief few minutes. Considering that concentrations of essential substrates may be quite disproportionate, the bulk of minor substrates, such as aromatic amino acids, could be lost to excretion while dominant substrates occupy a universal transport mechanism. Thus, duplication followed by strong specialization for the transport of indole- and phenyl-branched substrates is the key adaptation, which leads to a more efficient profile of nutrient absorption consistent with survival and rapid development of mosquito larvae under the pressure of limited nutrients.

(2) Why do mosquitoes possess spatial differences in the relative expression of aromatic AgNATs in the posterior midgut rather than expressing both transporters in identical epithelial loci or cells? The answer appears to be that the separation may reduce AgNAT competition for electrochemical energy and inorganic cation driving forces. Perhaps for the same reason, the membrane sector through which AgNAT6 absorbs the typically scarcer tryptophan is remarkably larger than the sector through which AgNAT8 absorbs the three to four times more concentrated phenylalanine and tyrosine substrates (based on the frequency of these amino acids in protein sequences). More generally, modulation of the relative

expression of NATs with distinct substrate profiles in the alimentary canal may be an important facet of physiological and genetic adaptation of an organism to a nutrient chain with a limited source of essential amino acids. It is therefore reasonable to propose that duplication, specialization, and morphological segregation are major steps in NATs adaptation and evolution.

Role of the AgNAT6–AgNAT8 duet in secretory epithelia

In addition to their role in housekeeping protein synthesis, insects use large amounts of aromatic substrates during ecdysis (Sugumaran, 2000), cuticle hardening and tanning (Sugumaran and Nelson, 1998; Vincent, 2002), egg chorion formation (Li, 1994); wound healing (Galko and Krasnow, 2004; Shi et al., 2006), immunity (Siva-Jothy and Thompson, 2002), melanotic encapsulation of pathogens (Hillyer et al., 2003; Koella and Sorensen, 2002), neurotransmission (Caveney and Donly, 2002; Osborne, 1996) and hormonal signaling (Gade and Goldsworthy, 2003; Kelly et al., 1994). Hence the demand for aromatic substrates is expected to be accompanied by an elevated expression of aromatic NATs. High densities of both AgNATs were identified in anterior domains of the larval alimentary canal, including salivary glands, cardia, gastric caeca and some areas of AMG (Fig. 4). Earlier we proposed that the gain of aromatic NAT transcription in the anterior region of the larval alimentary canal may support secretory functions of this region, e.g. secretion of peritrophic polymer precursors and salivary enzymes (Meleshkevitch et al., 2006). The location of aromatic NATs on the basal membrane of epithelial cell in the secretory region provides them with access to the large pool of free amino acids in the hemolymph. Strong support for this hypothesis is the unequivocal basal localization of both aromatic transporters in the salivary glands (Figs 5 and 6). Intriguing differences in the expression of AgNAT6 and AgNAT8 are found in other anterior structures. Thus AgNAT8, but not AgNAT6, is highly expressed in the cardia (Figs 5 and 6). This difference may reflect the high consumption of phenyl-branched substrates associated with phenol oxidase-mediated polymerization of peritrophic membrane peptides (Tellam et al., 1999). The opposite polarity of AgNAT6 and AgNAT8 suggests sorting of aromatic substrates in the gastric caeca. Perhaps it favors the absorption of indole substrates in parallel with the secretion of phenyl-branched components. The bipolar expression of AgNAT6 in the anterior midgut may correspond to an extensive turnover of alkalinization-maintaining components in this area. However, it may also imply the lack of a protein polar docking mechanism in this area of transient functional specialization. The variety of NATs expression has been demonstrated in different mammalian tissues using PCR (Broer et al., 2004; Broer et al., 2006b; Kowalczuk et al., 2005; Takanaga et al., 2005a; Takanaga et al., 2005b) and antibodies (Romeo et al., 2006). However, the alternative polarizations and spatial expression patterns of NATs in the functionally different parts of the metazoan alimentary canal are shown here for the first time. Although the mechanisms of relative expression and alternative polar docking of NATs remains to be clarified, the facts reported here establish the principal role of two NATs in the redistribution of essential aromatic substrates. The spatial tuning of expression and trafficking of individual NATs in the epithelial tissue may be a particular example of a more fundamental mechanism for functional pattern generation in the absorption of essential amino acid in different metazoan tissues and cells.

Upon analysis of electrophoretic migration patterns we identified different apparent molecular masses to the theoretically predicted masses of heterologously and tissue produced AgNATs (Fig. 1; theoretical pI/Mw are 6.85/72 772 and 7.06/70 233 for AgNAT6 and AgNAT8, respectively). Such a pattern suggests a posttranslational modification of the proteins, by either oligomerization, glycosylations or other posttranslational modifications of protein structure. Apparent scattering of the band migration pattern, probably as a result of glycosylation, was observed. In addition, two bands corresponded approximately to

calculated molecular masses of putative monomers and homodimers for each of the analyzed proteins. AgNAT6 and AgNAT8 have two and one putative glycosylation sites with position/probability being 200/0.76, 215/0.74 and 233/0.65, respectively. We suggest that the observed upper bands may correspond to homodimer formation because heavy glycosylation would reduce the migration of such proteins by ~10–20 kDa but not 50 kDa. The upper bands are predominant in the gut tissues but not in the heterologous expression system (Fig. 1) suggesting that the putative homodimers are the prevalent structure for both aromatic transporters in the gut tissues. The facts that symmetrical dimers were identified in other member of SLC6 by similar analysis (Hastrup et al., 2001), by FRET (Bossi et al., 2007) and upon crystallization of bacterial NAT AaLeuT (Yamashita et al., 2005) supports our hypothesis and suggests that dimer formation is conserved and essential for the physiological role of SLC6 members. A detailed analysis would be required to determine the exact nature and functional roles of quaternary modifications of NATs.

Integration of AgNATs in ion recycling pathways

Our previous electrophysiological analysis showed that both aromatic AgNATs use membrane potentials to drive Na^+- or K^+-coupled amino acid symport (Boudko et al., 2005a; Meleshkevitch et al., 2006). Both of these ions are at low concentrations in the freshwater habitat of *An. gambiae* larvae. The alkalinization to pH >10 of larval AMG involves the luminal resorption of chloride anions and secretion of strong cations, such as Na^+ or K^+ (Boudko et al., 2001a; Corena et al., 2001). The high pH has long been associated with digestion of nutrients and protection from pathogens in mosquito larvae (Clements, 1992). It is reasonable to propose that AMG alkalinization is also part of Na^+ and K^+ recycling, which provides NATs in the PMG with an essential pool of alkali metal ions (Fig. 6). As key users of cation gradients in the PMG, NATs complete a systemic loop for cation recycling between hemolymph and AMG. MT and the rectal gland are important components of a mineral cation recycling framework in freshwater mosquitoes (Smith et al., 2007) and may support cation recycling under low nutrient conditions, when NAT activity would be reduced. Alkali metal cations are replaced in the midgut lumen through the alkalinization that is mediated by basal H^+ V-ATPase in synergy with putative cation secretion and anion absorption mechanisms (Linser et al., 2007; Zhuang et al., 1999). Upon saturation of a luminal cation pool the NAT function can be energized by apical H^+ V-ATPase in the larval PMG. The H^+ V-ATPase hydrolyses ATP to move protons (H^+) outwardly across the cell membrane thereby hyperpolarizing the apical membranes; the resulting transmembrane voltage generates electrophoretic forces sufficient for inward movement of Na^+ and perhaps K^+ (considering that the apical K^+ reversal potential is relatively high) through apical membranes of epithelial cells. NATs couple the translocation of alkali metal cations to that of neutral amino acids. Thus, the H^+ V-ATPase is probably the most important source of electromotive force for the electrochemical coupling of NATs to metabolic energy in mosquitoes, as it is in caterpillars (Gluck, 1992; Harvey, 1992; Zhuang et al., 1999). However, this primary membrane energization *via* proton efflux would be incomplete without electrical coupling to secondary alkali metal translocation that in turn is coupled by NATs to tertiary amino acid translocation. For instance, the action of an electrophoretic cation/nH^+ antiporter coupled to a H^+ V-ATPase activity would be essential to support luminal secretion of sodium and potassium ions. Potentially Na^+, K^+-ATPase can be involved as well in the localized energization of NAT functions. Being located apically in the AMG and basally in the PMG (Okech et al., 2008) it would sustain an inward Na^+ gradient that would provide ions for Na^+-coupled amino acid absorption in the epithelial cells by exchanging intracellular Na^+ for K^+ (Castagna et al., 1998). Indeed, studies on other insect species have demonstrated the interaction of amino acid absorption with a basally located Na^+, K^+-ATPase (Castagna et al., 1998; Goberdhan et al., 2005; Mbungu et al.,

1995). Therefore, it seems reasonable that both, Na^+, K^+-ATPase-energized and (Na^+ or K^+), H^+ antiporter-H^+ V-ATPase-energized mechanisms support NAT function.

Acknowledgments

We thank MR4 for supplying *An. gambiae* eggs (the G3 strain was deposited by Dr Mark Benedict). This research was supported in part by NIH-NIAID research grant 5R01 AI-030464 (D.Y.B.) and by the Whitney Laboratory for Marine Bioscience (Dr Peter A. V. Anderson, Director).

LIST OF ABBREVIATIONS

AgNAT6	*An. gambiae* nutrient amino acid transporter 6 (tryptophan/indole-branched substrate transporter)
AgNAT8	*An. gambiae* nutrient amino acid transporter 8 (phenylalanine/phenyl-branched substrate transporter)
AMG	anterior midgut
CM	central midgut
DW	deionized water
FRET	fluorescence resonance energy transfer
GC	gastric caeca
MT	Malpighian tubules
NAT(s)	nutrient amino acid transporter(s)
PMG	posterior midgut
SG	salivary gland
SLC6	solute carrier family 6
SNF	sodium neurotransmitter symporter family

References

Assis P, Boudko DY, Meleshkevitch EA, Phung E. Molecular expression and electrochemical analysis of phenylalanine-tyrosine transporter from *Anopheles gambiae* larvae. FASEB J. 2004; 18:A1269.

Bohmer C, Broer A, Munzinger M, Kowalczuk S, Rasko JEJ, Lang F, Broer S. Characterization of mouse amino acid transporter B(0)AT1 (slc6a19). Biochem J. 2005; 389:745–751. [PubMed: 15804236]

Bossi E, Soragna A, Miszner A, Giovannardi S, Frangione V, Peres A. Oligomeric structure of the neutral amino acid transporters KAAT1 and CAATCH1. Am J Physiol. 2007; 292:C1379–C1387.

Boudko DY, Moroz LL, Harvey WR, Linser PJ. Alkalinization by chloride/bicarbonate pathway in larval mosquito midgut. Proc Natl Acad Sci USA. 2001a; 98:15354–15359. [PubMed: 11742083]

Boudko DY, Moroz LL, Linser PJ, Trimarchi JR, Smith PJS, Harvey WR. *In situ* analysis of pH gradients in mosquito larvae using noninvasive, self-referencing, pH-sensitive microelectrodes. J Exp Biol. 2001b; 204:691–699. [PubMed: 11171351]

Boudko DY, Kohn AB, Meleshkevitch EA, Dasher MK, Seron TJ, Stevens BR, Harvey WR. Ancestry and progeny of nutrient amino acid transporters. Proc Natl Acad Sci USA. 2005a; 102:1360–1365. [PubMed: 15665107]

Boudko DY, Meleshkevitch EA, Harvey WR. Novel transport phenotypes in the sodium neurotransmitter symporter family. FASEB J. 2005b; 19:A748.

Boudko, DY.; Stevens, BR.; Donly, BC.; Harvey, WR. Nutrient amino acid and neurotransmitter transporters. In: Iatrou, K.; Gill, SS.; Gilbert, LI., editors. Comprehensive Molecular Insect Science. Vol. 4. Amsterdam: Elsevier; 2005c. p. 255-309.

Bradford MM. A rapid and sensitive method for the quantitation of microgram quantities of protein utilizing the principle of protein-dye binding. Anal Biochem. 1976; 72:248–254. [PubMed: 942051]

Broer A, Klingel K, Kowalczuk S, Rasko JEJ, Cavanaugh J, Broer S. Molecular cloning of mouse amino acid transport system B-0, a neutral amino acid transporter related to Hartnup disorder. J Biol Chem. 2004; 279:24467–24476. [PubMed: 15044460]

Broer A, Cavanaugh JA, Rasko JEJ, Broer S. The molecular basis of neutral aminoacidurias. Pflugers Arch. 2006a; 451:511–517. [PubMed: 16052352]

Broer A, Tietze N, Kowalczuk S, Chubb S, Munzinger M, Bak LK, Broer S. The orphan transporter v7-3 (slc6a15) is a Na^+-dependent neutral amino acid transporter (B0AT2). Biochem J. 2006b; 393:421–430. [PubMed: 16185194]

Broer S. Adaptation of plasma membrane amino acid transport mechanisms to physiological demands. Pflugers Arch. 2002; 444:457–466. [PubMed: 12136264]

Broer S. The SLC6 orphans are forming a family of amino acid transporters. Neurochem Int. 2006; 48:559–567. [PubMed: 16540203]

Caccia S, Leonardi MG, Casartelli M, Grimaldi A, de Eguileor M, Pennacchio F, Giordana B. Nutrient absorption by *Aphidius ervi* larvae. J Insect Physiol. 2005; 51:1183–1192. [PubMed: 16085087]

Castagna M, Shayakul C, Trotti D, Sacchi V, Harvey W, Hediger M. Molecular characteristics of mammalian and insect amino acid transporters: implications for amino acid homeostasis. J Exp Biol. 1997; 200:269–286. [PubMed: 9050235]

Castagna M, Shayakul C, Trotti D, Sacchi VF, Harvey WR, Hediger MA. Cloning and characterization of a potassium-coupled amino acid transporter. Proc Natl Acad Sci USA. 1998; 95:5395–5400. [PubMed: 9560287]

Caveney, S.; Donly, BC. Neurotransmitter transporters in the insect nervous system. In: Evans, P., editor. Advances in Insect Physiology. Vol. 29. London: Academic Press; 2002. p. 55-149.

Clark TM, Vieira MAL, Huegel KL, Flury D, Carper M. Strategies for regulation of hemolymph pH in acidic and alkaline water by the larval mosquito *Aedes aegypti* (L.) (Diptera; Culicidae). J Exp Biol. 2007; 210:4359–4367. [PubMed: 18055625]

Clements, AN. The Biology of Mosquitoes. London: Chapman & Hall; 1992.

Corena MD, Linser PJ, Boudko D, Harvey WR, Seron TJ. Carbonic anhydrase and its role in the alkalinization mechanism of larval *Aedes aegypti* midgut. Mol Biol Cell. 2001; 12:390A.

Feldman DH, Harvey WR, Stevens BR. A novel electrogenic amino acid transporter is activated by K^+ or Na^+, is alkaline pH-dependent, and is Cl^--independent. J Biol Chem. 2000; 275:24518–24526. [PubMed: 10829035]

Gade G, Goldsworthy GJ. Insect peptide hormones: a selective review of their physiology and potential application for pest control. Pest Manag Sci. 2003; 59:1063–1075. [PubMed: 14561063]

Galko MJ, Krasnow MA. Cellular and genetic analysis of wound healing in *Drosophila* larvae. PLoS Biol. 2004; 2:1114–1126.

Giordana B, Sacchi VF, Parenti P, Hanozet GM. Amino acid transport systems in intestinal brush-border membranes from lepidopteran larvae. Am J Physiol. 1989; 257:R494–R500. [PubMed: 2675638]

Gluck S. V-ATPases of the plasma membrane. J Exp Biol. 1992; 172:29–37. [PubMed: 1491228]

Goberdhan DC, Meredith D, Boyd CA, Wilson C. PAT-related amino acid transporters regulate growth via a novel mechanism that does not require bulk transport of amino acids. Development. 2005; 132:2365–2375. [PubMed: 15843412]

Harvey WR. Physiology of V-ATPases. J Exp Biol. 1992; 172:1–17. [PubMed: 1491219]

Hastrup H, Karlin A, Javitch JA. Symmetrical dimer of the human dopamine transporter revealed by cross-linking Cys-306 at the extracellular end of the sixth transmembrane segment. Proc Natl Acad Sci USA. 2001; 98:10055–10060. [PubMed: 11526230]

Hill WG, Southern NM, MacIver B, Potter E, Apodaca G, Smith CP, Zeidel ML. Isolation and characterization of the *Xenopus* oocyte plasma membrane: a new method for studying activity of water and solute transporters. Am J Physiol. 2005; 289:F217–F224.

Hillyer JF, Schmidt SL, Christensen BM. Rapid phagocytosis and melanization of bacteria and plasmodium sporozoites by hemocytes of the mosquito *Aedes aegypti*. J Parasitol. 2003; 89:62–69. [PubMed: 12659304]

Hoglund PJ, Adzic D, Scicluna SJ, Lindblom J, Fredriksson R. The repertoire of solute carriers of family 6, identification of new human and rodent genes. Biochem Biophys Res Commun. 2005; 336:175–189. [PubMed: 16125675]

Holt RA, Subramanian GM, Halpern A, Sutton GG, Charlab R, Nusskern DR, Wincker P, Clark AG, Ribeiro JM, Wides R, et al. The genome sequence of the malaria mosquito *Anopheles gambiae*. Science. 2002; 298:129–149. [PubMed: 12364791]

Kelly, TJ.; Masler, EP.; Menn, JJ. Insect neuropeptides-current status and avenues for pest-control. In: Hedin, PA.; Menn, JJ.; Hollingworth, RM., editors. Natural and Engineered Pest Management Agents (ACS Symposium Series No 551). Washington, DC: American Chemical Society; 1994. p. 292-318.

Koella JC, Sorensen FL. Effect of adult nutrition on the melanization immune response of the malaria vector *Anopheles stephensi*. Med Vet Entomol. 2002; 16:316–320. [PubMed: 12243233]

Kowalczuk S, Broer A, Munzinger M, Tietze N, Klingel K, Broer S. Molecular cloning of the mouse IMINO system: an Na^+- and Cl^--dependent proline transporter. Biochem J. 2005; 386:417–422. [PubMed: 15689184]

Li JY. Egg chorion tanning in *Aedes aegypti* mosquito. Comp Biochem Physiol. 1994; 109A:835–843.

Linser PJ, Boudko DY, Corena Mdel P, Harvey WR, Seron TJ. The molecular genetics of larval mosquito biology: a path to new strategies for control. J Am Mosq Control Assoc. 2007; 23:283–293. [PubMed: 17853613]

Mbungu D, Ross LS, Gill SS. Cloning, functional expression, and pharmacology of a GABA transporter from *Manduca sexta*. Arch Biochem Biophys. 1995; 318:489–497. [PubMed: 7733681]

Meleshkevitch EA, Assis-Nascimento P, Popova LB, Miller MM, Kohn AB, Phung EN, Mandal A, Harvey WR, Boudko DY. Molecular characterization of the first aromatic nutrient transporter from the sodium neurotransmitter symporter family. J Exp Biol. 2006; 209:3183–3198. [PubMed: 16888066]

Nedergaard S. Active transport of α-aminoisobutyric acid by the isolated midgut of *Hyalophora cecropia*. J Exp Biol. 1972; 56:167–172.

Okech BA, Boudko DY, Harvey WR. Cationic pathway of pH regulation in larvae of *Anopheles gambiae*. J Exp Biol. 2008; 211:957–968. [PubMed: 18310121]

Osborne RH. Insect neurotransmission: neurotransmitters and their receptors. Pharmacol Ther. 1996; 69:117–142. [PubMed: 8984507]

Rheault MR, Okech BA, Keen SB, Miller MM, Meleshkevitch EA, Linser PJ, Boudko DY, Harvey WR. Molecular cloning, phylogeny and localization of AgNHA1: the first Na^+/H^+ antiporter (NHA) from a metazoan, *Anopheles gambiae*. J Exp Biol. 2007; 210:3848–3861. [PubMed: 17951426]

Romeo E, Dave MH, Bacic D, Ristic Z, Camargo SM, Loffing J, Wagner CA, Verrey F. Luminal kidney and intestine SLC6 amino acid transporters of B0AT-cluster and their tissue distribution in *Mus musculus*. Am J Physiol. 2006; 290:F376–F383.

Shi L, Li B, Paskewitz SM. Cloning and characterization of a putative inhibitor of melanization from *Anopheles gambiae*. Insect Mol Biol. 2006; 15:313–320. [PubMed: 16756550]

Siva-Jothy MT, Thompson JJW. Short-term nutrient deprivation affects immune function. Physiol Entomol. 2002; 27:206–212.

Smith KE, Vanekeris LA, Linser PJ. Cloning and characterization of AgCA9, a novel {alpha}-carbonic anhydrase from *Anopheles gambiae* Giles *sensu stricto* (Diptera: Culicidae) larvae. J Exp Biol. 2007; 210:3919–3930. [PubMed: 17981859]

Sugumaran M. Oxidation chemistry of 1,2-dehydro-N-acetyldopamines: direct evidence for the formation of 1,2-dehydro-N-acetyldopamine quinone. Arch Biochem Biophys. 2000; 378:404–410. [PubMed: 10860558]

Sugumaran M, Nelson E. Model sclerotization studies. 4 Generation of N-acetylmethionyl catechol adducts during tyrosinase-catalyzed oxidation of catechols in the presence of N-acetylmethionine. Arch Insect Biochem Physiol. 1998; 38:44–52. [PubMed: 9589603]

Takanaga H, Mackenzie B, Peng JB, Hediger MA. Characterization of a branched-chain amino-acid transporter SBAT1 (SLC6A15) that is expressed in human brain. Biochem Biophys Res Commun. 2005a; 337:892–900. [PubMed: 16226721]

Takanaga H, Mackenzie B, Suzuki Y, Hediger MA. Identification of mammalian proline transporter SIT1 (SLC6A20) with characteristics of classical system imino. J Biol Chem. 2005b; 280:8974–8984. [PubMed: 15632147]

Tellam RL, Wijffels G, Willadsen P. Peritrophic matrix proteins. Insect Biochem Mol Biol. 1999; 29:87–101. [PubMed: 10196732]

Thimgan MS, Berg JS, Stuart AE. Comparative sequence analysis and tissue localization of members of the SLC6 family of transporters in adult *Drosophila melanogaster*. J Exp Biol. 2006; 209:3383–3404. [PubMed: 16916974]

Uchida K, Ohmori D, Yamakura F, Suzuki K. Changes in free amino acid concentration in the hemolymph of the female *Culex pipiens* pallens (Diptera: Culicidae), after a blood meal. J Med Entomol. 1990; 27:302–308. [PubMed: 2332874]

Uchida K, Oda T, Matsuoka H, Moribayashi A, Ohmori D, Eshita Y, Fukunaga A. Induction of oogenesis in mosquitoes (Diptera: Culicidae) by infusion of the hemocoel with amino acids. J Med Entomol. 2001; 38:572–575. [PubMed: 11476338]

Uchida K, Moribayashi A, Matsuoka H, Oda T. Effects of mating on oogenesis induced by amino acid infusion, amino acid feeding, or blood feeding in the mosquito *Anopheles stephensi* (Diptera: Culicidae). J Med Entomol. 2003; 40:441–446. [PubMed: 14680108]

Verrey F, Ristic Z, Romeo E, Ramadan T, Makrides V, Dave MH, Wagner CA, Camargo SM. Novel renal amino acid transporters. Annu Rev Physiol. 2005; 67:557–572. [PubMed: 15709970]

Vincent JFV. Arthropod cuticle: a natural composite shell system. Composites Part A. 2002; 33:1311–1315.

Wolfersberger MG. Amino acid transport in insects. Annu Rev Entomol. 2000; 45:111–120. [PubMed: 10761572]

Yamashita A, Singh SK, Kawate T, Jin Y, Gouaux E. Crystal structure of a bacterial homologue of Na^{+}/Cl^{-}-dependent neurotransmitter transporters. Nature. 2005; 437:215–223. [PubMed: 16041361]

Zhang Z, Nichols JW. Protein-mediated transfer of fluorescent-labeled phospholipids across brush border of rabbit intestine. Am J Physiol. 1994; 267:G80–G86. [PubMed: 8048534]

Zhuang Z, Linser PJ, Harvey WR. Antibody to H(+) V-ATPase subunit E colocalizes with portasomes in alkaline larval midgut of a freshwater mosquito (*Aedes aegypti*). J Exp Biol. 1999; 202:2449–2460. [PubMed: 10460732]

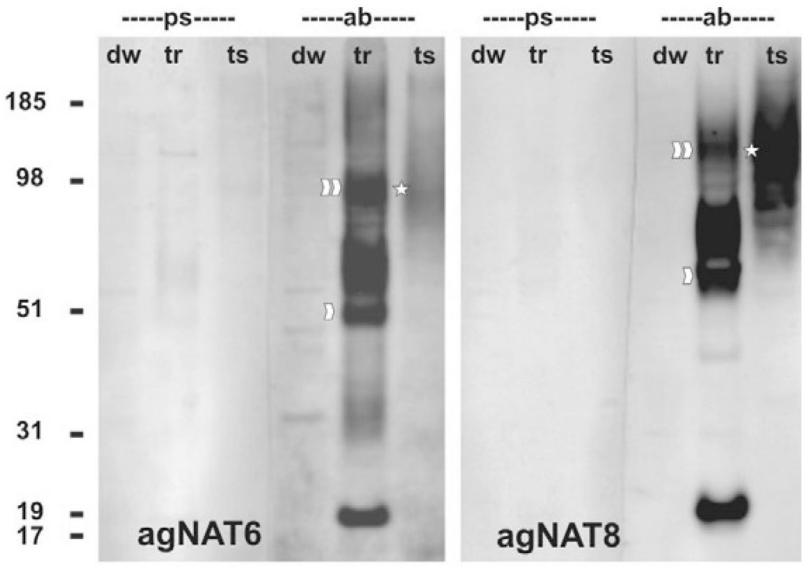

Fig. 1.

Western blot of AgNATs expression in *Xenopus* eggs and larval midgut tissues. Western blot analysis of AgNAT6 and AgNAT8 expression are shown in left and right panels, respectively. Lanes: ps, pre-immune sera; ab, purified antibodies; dw, tr and ts, membrane fractions from deionized water- or transcript-injected oocytes and midgut tissue, respectively. Numbers are protein mass references (in kDa). Arrowheads indicate putative monomer and homodimer bands. Asterisks indicate dimers in the tissue fractions.

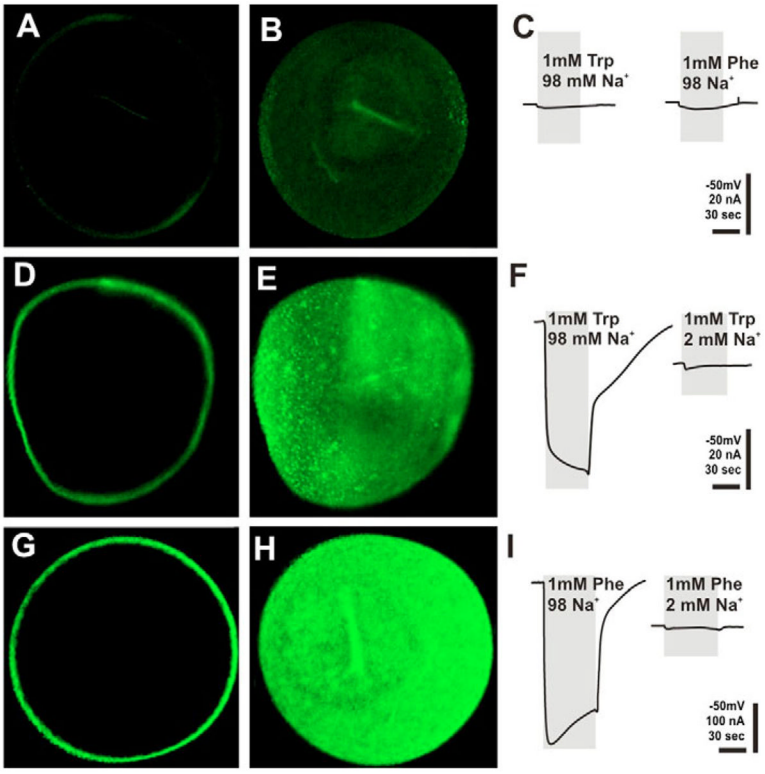

Fig. 2.

Functional expression of AgNAT6 and AgNAT8 in *Xenopus* oocytes. Images represent results of immunolabeling of oocytes with transporter-specific antibodies after oocytes were injected with (A,B) deionized water or (D–H) specific aromatic NAT transcripts, i.e. AgNAT6 (D,E) and AgNAT8 (G,H). Fourth day post-injection oocytes are shown. Control oocytes treated with AgNAT8 antibodies (A,B) and AgNAT6 antibodies (data not shown) produce very low background labeling. Optical mid-oocyte sections (A,D,G) and surface reconstruction from multiple confocal frames (B,E,H) are shown along with amino acid-induced currents (C,F,I).

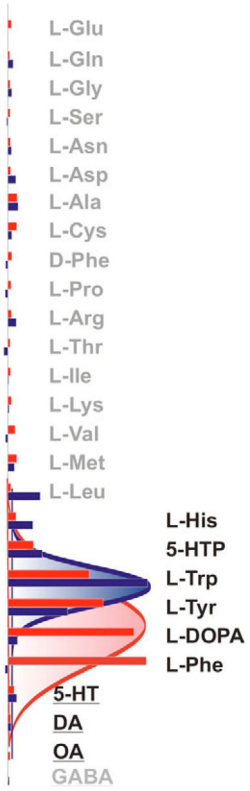

Fig. 3.

Relative transport efficiency of aromatic NATs. Normalized means (bars) of selected substrate-induced currents were acquired from independent oocytes ($N \geq 3$ for each data point). All responses were measured using standard conditions (98 mmol·l^{-1} Na^+ oocyte perfusion saline, 50 mV holding potential, and 1 mmol·l^{-1} of organic substrate concentrations). Data sets for AgNAT6 (blue set) and AgNAT8 (red set) were normalized relative to Trp- and Phe-induced responses and sorted with respect to amplitudes of induced currents and chemical substrate properties. Final data sets were fitted using a four parameters Gaussian pick function: $f=y0+a\exp\{-0.5[(x-x0)/b]\text{^}2\}$ indicated by red and blue lines. Substrate groups are indicated by different font styles: neurotransmitter, underlined; aromatic substrates, solid black; and all others gray.

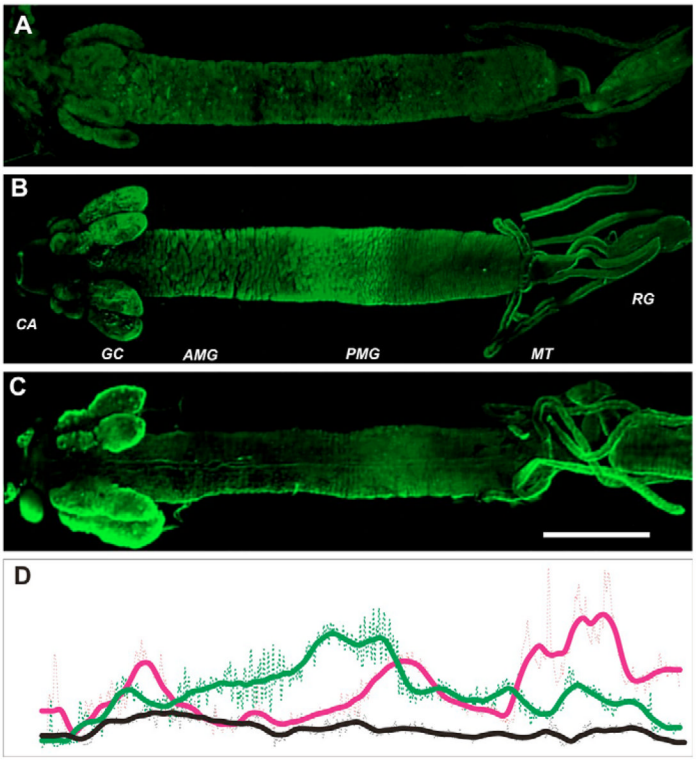

Fig. 4.

Relative distribution of AgNAT6 and AgNAT8 in the larval alimentary canal. Isolated alimentary canal of fourth instar larvae were labeled with (A) preimmune serum, (B) AgNAT6- and (C) AgNAT8-specific antibodies. Primary antibody binding areas were visualized using Alexa Fluor 467 secondary antibodies, producing green fluorescent signals. CA, cardia; GC, gastric caeca; AMG, anterior midgut; PMG, posterior midgut; MT, Malpighian tubes; RG, rectal gland. (D) Relative fluorescence intensities are shown along the larval alimentary canal (scans from A,B,C are represented by black, green and magenta lines, respectively). Rectangular area scan signal values are indicated by dotted lines; scans filtered by running average values indicated by solid lines. Scale bar, 1 mm.

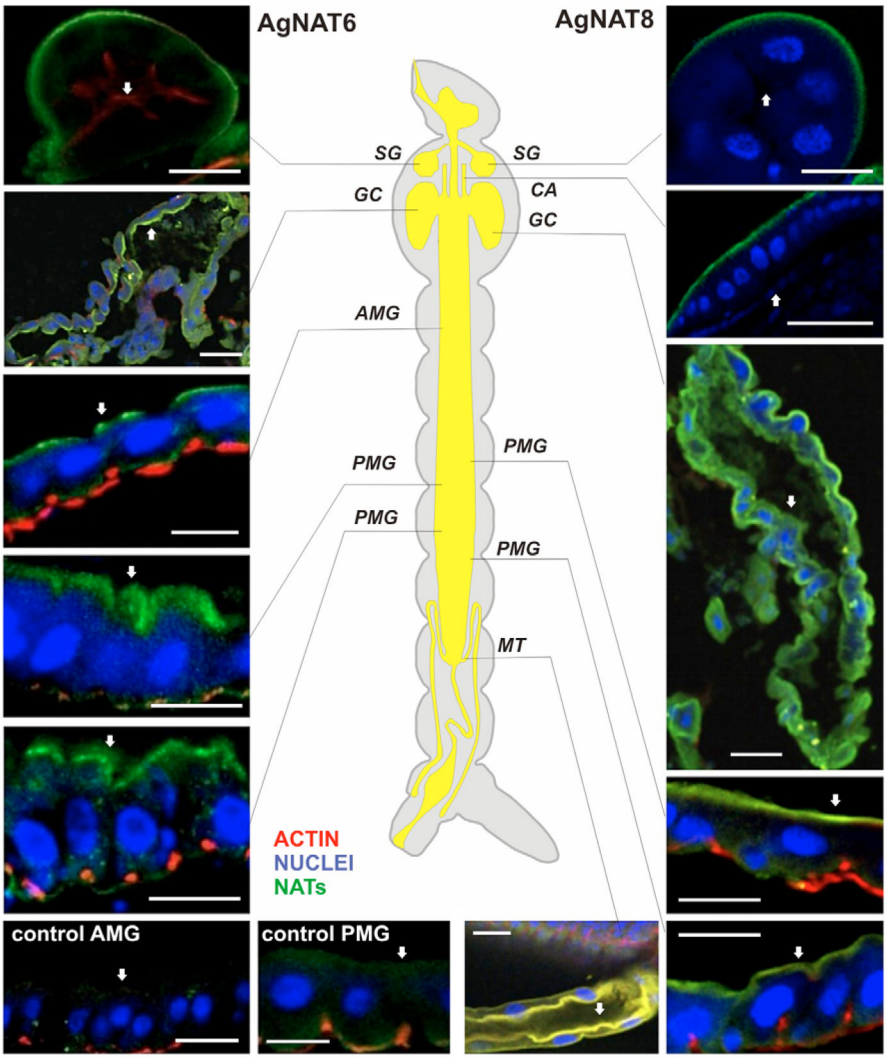

Fig. 5.

Immunolabeling of AgNATs on frozen sections of the larval alimentary canal. Immunolabeling of frozen sections with AgNAT6 (left site of the panel) AgNAT8 (right site of the panel) epitope-specific purified antibodies (green channel), along with actin (TRITC-phalloidin, red channel)- and nuclei (DRAQ-5, blue channel)-specific labeling are shown. The actin and nuclei channels were turn off on a few sections to improve overall visualization. The red channel in general represents actin of the muscular envelop around the gut, and corresponds to the position of the basal membrane, except in the salivary gland and Malpighian tubules where it indicates the actin of microvillae and the apical membrane, respectively. The position of the apical membrane is indicated by white arrows. Approximate positions of individual sections are shown on the central diagram. SG, salivary gland; CA, cardia; GC, gastric caeca; AMG, anterior midgut; PMG, posterior midgut; MT, Malpighian tubes. Control sections of the AMG (control AMG) and PMG (control PMG) incubated with pre-bleed serum are shown in the bottom left corner. Scale bars, 50 μm.

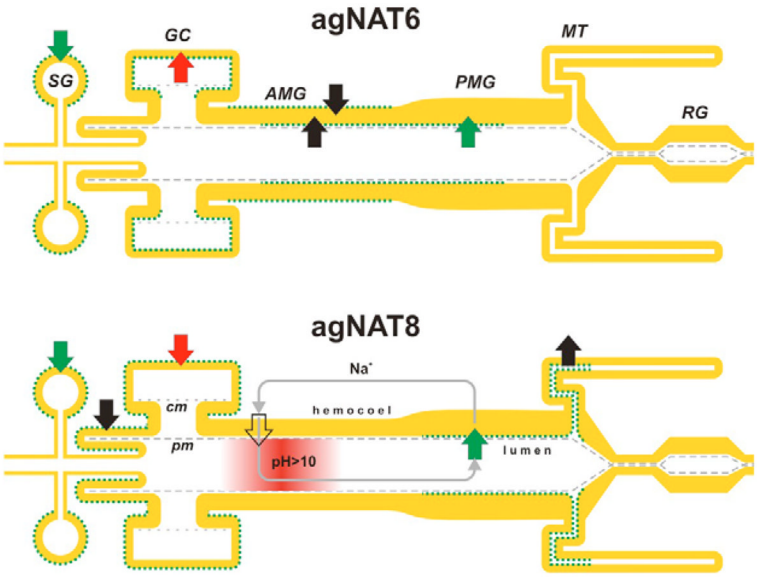

Fig. 6.

A diagram of the relative distribution of aromatic AgNATs in the model system of the larval alimentary canal. A summary diagram composed from whole-mount and frozen section preparations is shown (N>20 for each transporter). Green dotted lines indicate membrane docking of the transporters. Colored arrows indicate direction of transport at specified locations. Their colors show either the same (green), specific (black) and opposed directions of substrate transport by AgNAT6 (top part) compared with AgNAT8 (bottom part). Gray arrows show a putative circuit of cation recycling *via* alkalinization (pink gradient region) and NAT-coupled pathway. Empty arrow indicates location of a putative H^+ V-ATPase and cation exchanger-coupled mechanism for cation translocation in the AMG. SG, salivary gland; GC, gastric caeca; AMG, anterior midgut; PMG, posterior midgut; MT, Malpighian tubes; RG, rectal gland; cm, caecal membrane; pm, peritrophic membrane.